Catalysis Science & Technology

Heterogenization for polyoxometalates as solid catalysts in aerobic oxidation of glycerol

Journal:	*Catalysis Science & Technology*
Manuscript ID	CY-ART-03-2020-000403.R1
Article Type:	Paper
Date Submitted by the Author:	17-Feb-2020
Complete List of Authors:	Tao, Meilin; Key Lab of Polyoxometalate Science of Ministry of Education, Faculty of Chemistry li, yue; Northeast Normal University Li, Yiming; Northest Normal University Zhang, Xueyan; Northeast Normal University Geletii, Yurii; Emory University, Department of Chemistry Wang, Xiaohong; Northeast Normal University, Hill, Craig; Emory University, Department of Chemistry

ARTICLE

Heterogenization for polyoxometalates as solid catalysts in aerobic oxidation of glycerol

Meilin Tao,[a,b,c] Yue Li,[a,c] Yiming Li,[a] Xueyan Zhang,[a] Yurii V Geletii,[b] Xiaohong Wang,*[a] Craig L Hill*[b]

[a]Key Lab of Polyoxometalate Science of Ministry of Education, Northeast Normal University, Changchun 130024, P. R. China, E-mail: wangxh665@nenu.edu.cn.
[b]Department of Chemistry, Emory University, Atlanta, Georgia 30322, United States
[c]These authors contributed equally to this work

A series of heterogeneous catalysts based on phosphomolybdic salts with different metals in counter or substituent places $L_nPMo_{12}O_{40}$ (L = Al^{3+}, Fe^{3+}, Cr^{3+}, Ti^{4+}, Zr^{4+} and Zn^{2+}, abbreviated as $LPMo_{12}$) and $H_xPMo_{11}LO_{39}$ (L= Zn^{2+}, Cr^{3+}, Fe^{3+}, Al^{3+}, Ti^{4+}, for Ti^{4+}, the amount of O is 40, abbreviated as $HPMo_{11}L$) have been prepared using simple calcination treatment, which were evaluated in aerobic oxidation of glycerol. After calcination at about 250 °C for 4 h, homogeneous $L_nPMo_{12}O_{40} \cdot nH_2O$ and $H_xPMo_{11}LO_{39} \cdot mH_2O$ resulted to heterogeneousones. The specific surface areas were also enhanced, as well as activity and reusability. Similar as homogeneous ones, $AlPMo_{12}$ treated at 400 °C ($AlPMo_{12}$-400) was found to be the most active one in glycerol oxidation to lactic acid with 96.1 % yield at 98.6 % conversion at 60 °C for 5 h with 1 MPa of O_2, which gave turnover number TON (TON = [LA]/[catalyst]) as 2.4×10^2, higher than $AlPMo_{12}$-250 did (TON = 2.0×10^2) ($AlPMo_{12}$-250 means treated at 250 °C). $AlPMo_{12}$ behaved as heterogeneous one in glycerol oxidation, which could be reused at least 12 times.$AlPMo_{12}$-400also performed well in crude glycerol oxidation, which gave lactic acid yield as high as 86.8 %.

Introduction

Polyoxometalates (POMs) are a large family of metal-oxo-cluster polyanions with oxo-metal polyhedral MO_6 (M = Mo or W) as basic construction units. Their protonated forms known as heteropolyacids (HPAs) are very strong Brønsted acids, while also can be used as Lewis acids if certain metal ions are introduced to their primary or secondary structure.[1-6]Meanwhile, POMs are often regarded as electron reservoirs for redox transformation of organic substrates.[7] Importantly, the structures and properties of POMs could be altered through simple and common ways of changing compositions.[7] On this concept, POMs are good candidates for various catalysis including Brønsted acid, Lewis acid or redox catalysis, even their combinations.

Glycerol is a by-product in biodiesel production, which is one of the best feedstocks for preparation of lactic acid (LA).[8]Various materials were prepared to catalyze the conversion of glycerol (**Table S1**).Among all, Hutchings' group use 1 % Au/graphite or activated carbon as catalysts in glycerol oxidation, got 100 % selectivity to glyceric acid under mild reaction conditions (60 °C, 3 h).[9,10]Prati's group also got very good results (92% selectivity to glycerate at fullconversion) using gold on carbon as the catalyst (30 ◦C, with a NaOH/glycerol ratio of 4, a glycerol/Au = 500, and 0.3 M concentration).[11-13] these results are all impressive, however, NaOH was used as addition, which may corrode the instruments, and the usage of noble metals may limited their application. POMs were found to be the most active catalysts in oxidative transformation of glycerol into LA by our group.[14-20] Homogeneous POMs as $H_3PMo_{12}O_{40}$, $LPMo_{12}O_{40}$ or $H_xPMo_{11}LO_{39}$ (L = K^+, Zn^{2+}, Cu^{2+}, Al^{3+}, Cr^{3+}, and Fe^{3+}) were evaluated in this field to exhibit some catalytic activity in one-pot conversion of glycerol into LA due to their suitable redox potentials and coexistence of Brønsted acidity or Lewis ones. Compared to heterogeneous catalysis, homogeneous one mostly faced the drawbacks of separating and regeneration despite of its higher efficiency.[21] During the last decades, numerous reviews summarized the polyoxometalate heterogenezation.[22-24]The most classic one is Makoto Misono's report, which discussed that counter-cations greatly influence the tertiary structure of POMs. They replaced protons using large metal ions like Cs, NH_4, etc to generate heterogeneous POMs

with high surface areas. For example, the surface area of $Cs_{2.5}H_{0.5}PW_{12}O_{40}$is 135 m^2/g much higher than protonated $H_3PW_{12}O_{40}$(6 m^2/g).[23]Generally, POM-based heterogeneous catalysts can be prepared mainly by two strategies, namely "solidification" and "immobilization" of the catalytically active POMs on solid supports.[25-26] As shown in **Table S2**, the former one is to introduce metal ions such as Cs^+, Ag^+, K^+, NH_4^+ or quaternary ammonium salts to partial exchange proton to form new POMs,[27-32] while the latter one involves supporting the POM active species on various porous materials such as SBA-15, mesoporous silicon, macroporous resin, graphene, and mesoporous metal oxide.[33-36] The two strategies can not only heterogenize homogeneous catalysts, but also increase the specific surface area (SSA) and acidity of catalysts, hence accelerate the catalytic reaction rate. Our group also fabricated solid POMs through loading $H_3PMo_{12}O_{40}$ on carbon materials and graphene,[17-18] while the synthetic procedures were complicated. It is well known that POMs with H^+, Na^+, Al^{3+}, or lanthanide metal cations as counter ions are soluble in water because of their small ion sizes.[37] Therefore, changing these POMs into insoluble materials has great value and wide applications. As a continuation, we wanted to develop an easy way to prepare solid $LPMo_{12}O_{40}$ or $H_3PMo_{11}LO_{39}$ (L= Zn^{2+}, Cr^{3+}, Fe^{3+}, Al^{3+}, Ti^{4+}, for Ti^{4+}, the amount of O is 40) to permit them behave like heterogeneous catalysts.

Herein, we prepared a series of heterogeneous phosphomolybdic salts of $L_nPMo_{12}O_{40}$ (L = Al^{3+}, Fe^{3+}, Cr^{3+}, Ti^{4+}, Zr^{4+} and Zn^{2+}, abbreviated as $LPMo_{12}$) and mono-substituted POMs $H_xPMo_{11}LO_{39}$ (L= Zn^{2+}, Cr^{3+}, Fe^{3+}, Al^{3+}, Ti^{4+}, for Ti^{4+}, the amount of O is 40, abbreviated as $HPMo_{11}L$) through simply calcination dehydration treatment at different temperature. Being treated like this, soluble POMs will lose their water of crystallization or lattice water turning to insoluble ones. Furthermore, after being treated at 400 °C,POMs owned high specific surface area due to the formation of stacking mesoporous structure, which could provide a reactor for glycerol oxidation. Meanwhile, the pathways for glycerol conversion upon these solid POM catalysts were also investigated to compare with those on homogeneous ones to determine the influence of surface area, porous property, Lewis acidity and redox potentials on the reaction.

Experimental

Preparation of catalysts

The heterogeneous $LPMo_{12}$ catalysts were synthesized by an ion-exchanged method, according to the procedure described previously.[38-39] Firstly, 9.1 g (5 mmol) of $H_3PMo_{12}O_{40}$ was dissolved in 10 mL of deionized water at room temperature under vigorous stirring. Then, 5.0 mmol solutions of $CrCl_3$, $Fe(NO_3)_3$ and $AlCl_3$; or 3.75 mmol of $Ti(SO_4)_2$ or $ZrCl_4$ and 7.5 mmol of $ZnSO_4$ were added dropwise and the mixture was stirred for 1 h at room temperature. Then, a dropwise addition of dimethyl sulfoxide (DMSO) resulted in a formation of yellow precipitate (dark green for $CrPMo_{12}$). The precipitates were filtered and dried under nitrogen. Afterward, the powders were calcinated at 250 °C under N_2 flow for 4 h to obtain heterogeneous $LPMo_{12}$ with the yields around 76 %. The stoichiometry of cation exchange is in eqs 1-3.

$$0.75L^{4+}+H_3PMo_{12}O_{40}\rightarrow 3H^+ + L_{0.75}PMo_{12}O_{40}(L = Ti^{4+}, Zr^{4+}) \quad (1)$$

$$L^{3+} + H_3PMo_{12}O_{40}\rightarrow 3H^+ + L_{1.0}PMo_{12}O_{40}(L = Fe^{3+}, Al^{3+}, Cr^{3+}) \quad (2)$$

$$1.5\ L^{2+} + H_3PMo_{12}O_{40}\rightarrow 3H^+ + L_{1.5}PMo_{12}O_{40}\ \ (L = Zn^{2+}) \quad (3)$$

The $HPMo_{11}L$ catalysts were prepared according to the reference.[40] A mixture of H_2SO_4 (0.5 M, 50 mL), H_3PO_4 (1 M, 25.2 mL), metal salts aqueous solution (chlorides for Cr and Zn; nitrates for Fe; sulfate for Al and Ti) (1 M, 25 mL) and deionized water (25 mL) was added to 250 mL sodium heptamolybdate aqueous solution (1 M). In order to avoid 6-molybdometalate formation, the synthesis was carried out at 0 °C. Then, KCl was added to precipitate the salts. 2 g potassium salts of $KPMo_{11}L$ (L = Ti^{4+}, Al^{3+}, Fe^{3+}, Cr^{3+} and Zn^{2+}) were dissolved respectively in 1000 mL deionized water and then the potassium cations were replaced by H^+ using strong-acid cation exchange resins (Type 732, 20 g) for several times to give $HPMo_{11}L$, until no K^+ was detected by ICP analysis. After that, the powder was calcined at 250 °C in $N_2$for 4 h to loss their crystal water. The formation of $HPMo_{11}L$ reaction undergoes based on the following equations:

$$11MoO_4^{4-} + H_3PO_4 + 13H^+ + L^{x+} + (9-x)K^+\rightarrow K_{9-x}PMo_{11}LO_{40} + 8H_2O\ (L = Ti^{4+}) \quad (4)$$

$$11MoO_4^{4-} + H_3PO_4 + 15H^+ + L^{x+} + (9-x)K^+\rightarrow K_{9-x}PMo_{11}LO_{39} + 9H_2O\ (L = Al^{3+}, Fe^{3+}, Cr^{3+}\text{ and }Zn^{2+}) \quad (5)$$

$$K_{9-x}PMo_{11}LO_{40} + (9-x)H^+\rightarrow H_{9-x}PMo_{11}LO_{40}\ \ (L = Ti^{4+}) \quad (6)$$

$$K_{9-x}PMo_{11}LO_{39} + (9-x)H^+\rightarrow H_{9-x}PMo_{11}LO_{39}\ \ (L = Al^{3+}, Fe^{3+}, Cr^{3+}\text{ and }Zn^{2+}) \quad (7)$$

Catalytic experiment

Glycerol oxidation was performed in a high-pressure stainless-steel autoclave with a polytetrafluoroethylene insert (10 mL) at a constant temperature of 60 °C and 1 MPa O_2 pressure. We did not use buffered solutions since i) it would be unacceptable for industrial process; ii) the pH of solutions changes in a narrow range between 2 (pH of 1.0 M lactic acid solution) and 3 (natural pH of solutions loaded with a catalyst). The autoclave was connected to the O_2 supply system, which kept the pressure constant. The solution was stirred magnetically. Typically, 5.0 mL of 1.0 M glycerol in water was oxidized in the presence of 4.0 mM catalyst. After desired time, the reactor was quickly cooled down, depressurized and the catalyst was removed by centrifuging. The remaining solution was diluted 10 times with distilled water and analyzed by a high performance liquid chromatography (HPLC) using a Shimadzu LC10A-VP chromatograph equipped with SPB-10A UV and RID-10A R.I. detectors, and a Prevail TM C18 (4.6 mm × 250 mm) column. A solution of H_2SO_4 (0.1 % w/w) in H_2O/acetonitrile (1/2 v/v) was used as the eluent at a flow rate of 1.0 mL/min at 50 °C. The glycerol conversion, α, and the selectivity for lactic acid (LA), S_{LA}, were calculated using eqs 8-9:

$$\alpha = ([GLY]_0 - [GLY]) / [GLY]_0 \times 100\ \% \quad (8)$$

$$S_{LA} = [LA]/([GLY]_0 - [GLY]) \times 100\ \% \quad (9)$$

Results and discussion

1. Heterogenization of $LPMo_{12}$ and $HPMo_{11}L$

$LPMo_{12}O_{40} \cdot nH_2O$ and $H_nPMo_{11}LO_{40} \cdot mH_2O$ are both soluble in water acting as homogeneous catalysts in glycerol conversion (**Figure 1, Table 1**). TG and DTA of $AlPMo_{12}$ and $HPMo_{11}Al$ in a higher temperature (900 °C) were measured as shown in **Figure. S1**. The DTA curve of $AlPMo_{12}$ illustrated that there was an exothermic peak between 98.5 °C and 278.6 °C attributed to removing the crystal water (total 13 per $AlPMo_{12}$). The appearance of endothermic peak between 360.6 °C and 499.6 °C due to the loss of structure water (1.5 per $AlPMo_{12}$). The exothermic peaks after between 590.9 °C and 700 °C belonged to the decomposition of $[PMo_{12}O_{40}]^{3-}$Keggin structure to form phosphorous oxide and molybdenum compounds, which were highly consistent with the literature.[41] $MoO_3$and $P_2O_5$is distinctly volatile, so the large weight loss after 750 °C to 900 °C was attributed to the sublimation of molybdenum and phosphorus compounds.[42] The same phenomenon were also observed in the DTA of $HPMo_{11}Al$, while there was an exothermic peak between 72.8 °C to 252.1 °C due to the removing of most crystal water (10 per $HPMo_{11}Al$) and an endothermic peak between 412.5 °C and 545.5 °C due to the loss of lattice water (2.0 per $HPMo_{11}Al$). The exothermic peaks around 600- 701.1 °C belonged to the decomposition of $[PMo_{11}AlO_{39}]^{3-}$Keggin structure to form phosphorous oxide and molybdenum compounds. The large weight loss between 750 °C to 900 °C was also attributed to the sublimation of molybdenum and phosphorus compounds. Based on the TG test for $AlPMo_{12}$ and $HPMo_{11}Al$, the calcination temperatures were selected as 150, 200, and 250 °C, respectively. After calcination at the three temperatures for 4 h, the crystal water was removed as 9, 11, and 13, respectively, showing that the crystal water could be removed by thermal treatment at 250 °C for 4 h for $AlPMo_{12}$. Meanwhile, the heating treatment for $HPMo_{11}Al$ also gave the same results. Water molecules removed for $HPMo_{11}Al$ were 7, 9, and 10 after heating at 120, 150, and 250 °C. As the calcination temperature increased from 150 to 250 °C, based on the standard curve in UV-Vis spectra, the solubility of $AlPMo_{12}$ decreased from 0.500 g/L to 0.084 g/L at 60 °C (**Figure 1**). The same treatment for $HPMo_{11}Al$ was also resulted in its heterogenization as the solubility lowing from 0.251 g/L to 0.014 g/L with 18 times lowing (**Table 1**). The solubility as low as 0.084 and 0.014 g/L means that $AlPMo_{12}$ and $HPMo_{11}Al$ are insoluble in water at 60 °C.

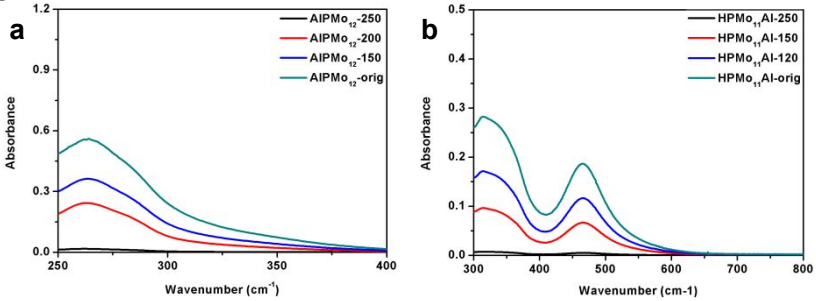

Figure 1. UV-Vis of $AlPMo_{12}$(a) and $HPMo_{11}Al$ (b) in water after calcinations in different temperatures.

The calcinations treatment for $AlPMo_{12}$ and $HPMo_{11}Al$ also changed the specific surface area as 4.6 m^2/g (treatment at 150 °C) < 5.9 m^2/g (200 °C) < 12.0 m^2/g (250 °C) for $AlPMo_{12}$, and 16.1 m^2/g (120 °C) < 17.8 m^2/g (150 °C) < 20.1 m^2/g (250 °C) for $HPMo_{11}Al$, respectively. Although the specific surface area was increased compared to their initial stage, it was not satisfied enough in catalytic reactions. Therefore, $AlPMo_{12}$ was calcinated at 400 °C. As results, the specific surface area and solubility were improved to 88.2 m^2/g and 0.012 g/L (**Table 1**, **Figure. S2**). It was found that after being treated at 400 °C,mesopores structure with 5.16 nm pore size was generateddue to the stacking of $AlPMo_{12}$, which could provide a reactor for glycerol oxidation**(Figure. S2**). Let's take $AlPMo_{12}$ as an example to illustrate the mechanism of mesopores structure. Based on the reports of Makoto Misono, [23]POMs inthe solid state have hierarchic structures: the primary structure is large polyanions, and the secondary structure is the three-dimensional arrangement of cations, crystal water, and other molecules". Recently, tertiary structure including the size of the particles, pore structure, distribution of protons in the particle, etc is found to be important to their catalytic activity of solid POMs. Firstly, after calcinations, the primary structure of $AlPMo_{12}$ did not change, while the mesopores appeared and surface area increased dramatically (**Figure S2**), which declared that the pores of POMs are interparticle, not intracrystalline. Probable preparation processes for $AlPW_{12}$-400 are schematically illustrated in **Scheme S1**.Before calcinations, ultra fine particles of $AlPW_{12}$ homogeneously dispersed in the solution. The N_2 sorption isotherms showed almost no adsorption. Heat treatment removed the water of crystallization and Lattice water, the particles stacked together to form mesopores and micropores. This phenomenon could be verified by the N_2 sorption isotherms of $AlPMo_{12}$-400 (**Figure S2**), in which adsorption happened in lower pressure, and hysteresis Loop appeared in higher temperature. The SEM image of $AlPMo_{12}$-400 (**Figure S3**) also showed the stacked morphology of catalyst after calcination treatment. In addition, the pore size distribution showed the pore sizes of catalysts were 5.16 nm for $AlPMo_{12}$-400, and 4.98 nm for $HPMo_{11}Al$-400. Both of them were larger than the sizes of glycerol and all the products, which avoided the influence of mass transfer restrictions, and guaranteed the smooth reaction.

Based on the TG analysis of $LPMo_{12}$ and $HPMo_{11}L$ (L = Zn^{2+}, Cr^{3+}, Fe^{3+}, Al^{3+}, Ti^{4+}) (**Figure S4**), heterogenization for these POMs was done through calcination at 250 °C for 4 h. And the structural integrity of homogeneous and heterogeneous catalysts was also characterized by elementary analysis, FTIR, XRD, and ^{31}P MAS NMR (**Figure S5-11, Table S3-4**). It can be concluded that soluble $LPMo_{12}$ and $HPMo_{11}L$ treated at 250 °Cto be dehydrated to insoluble ones, while their original keggin structure was kept. Meanwhile, dehydration at higher temperature such as 400 °C might result in enhancing BET surface area and generation of mesopores for solid POM salts.

Table 1. Glycerol conversion and selectivity to LA over $AlPMo_{12}$and $HPMo_{11}Al$ catalysts calcinated at different temperatures.

Entry	Catalysts	Specific surface area/$m^2 \cdot g^{-1}$	Solubility /$g \cdot L^{-1}$	Conversion/%	LA Yield/%	TOF/h^{-1}
1	$HPMo_{11}Al$-orig	12.4	0.251	55.6	28.0	14
2	$HPMo_{11}Al$-120	16.1	0.172	65.2	36.5	18.3
3	$HPMo_{11}Al$-150	17.8	0.102	71.8	44.2	22.1
4	$HPMo_{11}Al$-250	20.1	0.014	78.1	55.0	27.5
5	$HPMo_{11}Al$-450	79.1	0.008	87.5	70.3	35.2
5	$AlPMo_{12}$-orig	3.5	0.500	72.3	55.1	27.6
6	$AlPMo_{12}$-150	4.6	0.329	86.6	68.4	34.2
7	$AlPMo_{12}$-200	5.9	0.206	90.2	78.3	39.2
8	$AlPMo_{12}$-250	12.0	0.084	93.7	84.8	42.4
9	$AlPMo_{12}$-400	88.2	0.012	98.6	96.1	48.1

Reaction conditions: 5 mL, 1 M of glycerol, 4.0 mM of catalysts, 1 MPa of O_2, 800 rpm, 5 h.TOF = [LA]/[catalyst]·reaction time.

2. Scanning the activity of $LPMo_{12}$ and $HPMo_{11}L$ on glycerol conversion

The catalytic activity of $LPMo_{12}$ and $HPMo^{11}L$ was scanned in glycerol conversion in one-pot under reaction conditions as 5.0 mL, 1.0 M of glycerol, 4.0 mM catalysts, 1.0 MPa O_2, 800 rpm, 5 h (**Figure 2, Table S5-6**). The glycerol conversion depended on their compositions as $AlPMo_{12}$ (93.7 %) > $FePMo_{12}$ (90.0 %) > $CrPMo_{12}$ (88.2 %) > $TiPMo_{12}$ (77.0 %) > $ZrPMo_{12}$ (48.4 %) > $ZnPMo_{12}$ (30.1 %) and $HPMo_{11}Al$

(78.1 %) > $HPMo_{11}Fe$ (68.2 %) > $HPMo_{11}Ti$ (50.1 %) > $HPMo_{11}Cr$ (31.0 %) > $HPMo_{11}Zn$ (16.2 %), respectively. These activity orders were similar to their homogeneous forms,[16] indicating that the composition was the main contribution to glycerol conversion upon oxygen. High and suitable redox potentials for POM catalysts were essential for glycerol oxidation, which were measured by H_2-TPR (**Figure 3**). The peaks appeared around 500 °C for $LPMo_{12}$. And the H_2 consuming amounts based on peak area were $AlPMo_{12}$ (3.5×10^{-6} mol/mol) > $FePMo_{12}$ (3.1×10^{-6} mol/mol) > $CrPMo_{12}$ (2.8×10^{-6} mol/mol) > $TiPMo_{12}$ (2.4×10^{-6} mol/mol) > $ZrPMo_{12}$ (2.1×10^{-6} mol/mol) > $ZnPMo_{12}$ (1.7×10^{-6} mol/mol) > $H_3PMo_{12}O_{40}$ (1.5×10^{-6} mol/mol). The decrease of H_2 consuming and the shifts to higher temperature were attributed to the drop of oxidative ability. The same tracks were also observed in the H_2-TPR of $HPMo_{11}L$ series as $HPMo_{11}Al$ (5.3×10^{-6} mol/mol) > $HPMo_{11}Fe$ (4.8×10^{-6} mol/mol) > $HPMo_{11}Ti$ (4.3×10^{-6} mol/mol) > $HPMo_{11}Cr$ (3.6×10^{-6} mol/mol) > $HPMo_{11}Zn$ (3.2×10^{-6} mol/mol), which also declared that the H_2 adsorption amount increased with the growth of redox potentials of the materials. Based on the reports, [43, 44] the reduction peaks around 500 and 600 °C were ascribed to the reduction of molybdenum oxides originating from the destruction of polyanion.It was clear that the reduction degree and temperature strongly depended on the incorporation of metal species and their location. The peaks attributed to the substituted metals were too small to be seen, and the positions of reduction peaks and the corresponding peak areas changed as varying the metal ions either for $LPMo_{12}$ or for $HPMo_{11}L$. Therefore, the redox potentials of POMs can be controlled by changing the species of metal ions. To avoid the influence of metal content, we use the same mol of every catalyst.

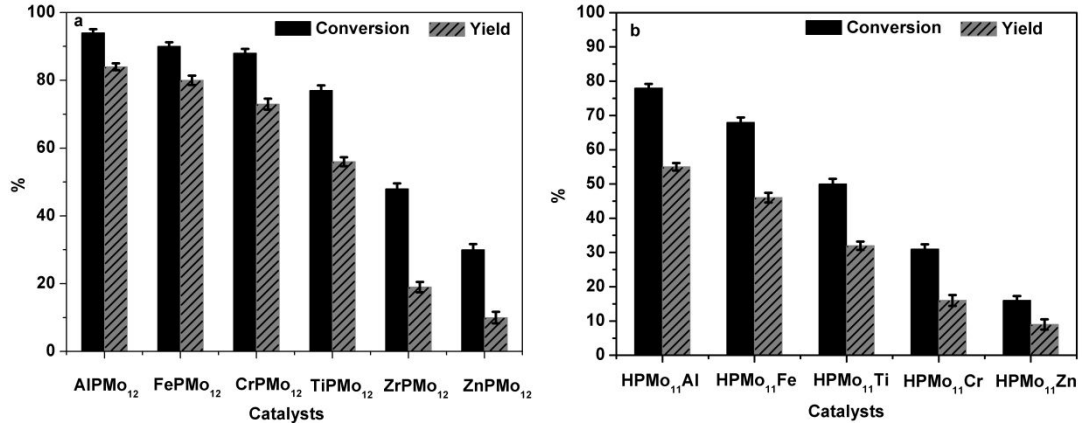

Figure 2. Catalytic activity of $LPMo_{12}$ and $HPMo_{11}L$ in glycerol oxidation: 1 M of glycerol, 4 mMof catalyst, 60 °C, 5 h, 1 MPa O_2, 800 rpm.

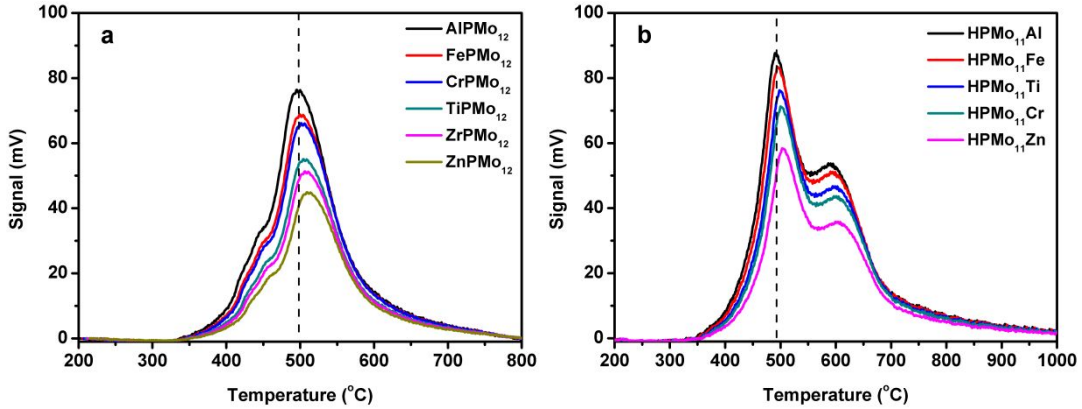

Figure3. The H_2-TPR spectra of $LPMo_{12}$ and $HPMo_{11}L$

In our or others' previous study,[16,21] glycerol undergoes a series of conversion into LA in the presence of O_2 including oxidation of glycerol to dihydroxyacetone (DHA) or glyceraldehydes (GCA) through a branching radical chain process (Eqs.10-11); isomerisation of GCA to DHA (Eq. 12); following by dehydration of DHA to pyruvaldehyde (PRA) (Eq. 13); final hydration of PRA to LA (Eq. 14).

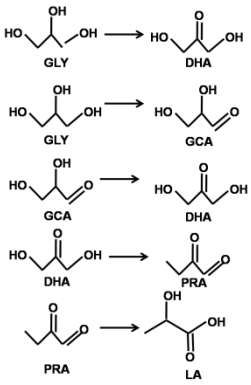

(10)

(11)

(12)

(13)

(14)

In order to obtain high yield of LA, the multiple active sites were required for catalysts as redox or Brønsted or Lewis acid ones.[45-46] For this purpose, a series of reactions in glycerol transformation upon $LPMo_{12}$ and $HPMo_{11}L$ were carried out to determine the effect of multi-centres on each pathway (**Table 2**). N_2 was used instead of O_2in the reaction to demonstrate O_2 was not essential in this step. The Lewis acidity and Brønsted acidity were tested and calculated by FTIR spectra of pyridine adsorption based on Lambert-Beer equation (**Figure S12**).[47] It can be seen that (1) in isomerisation of GCA to DHA, there was only 4.3 % GCA converted into DHA, showing that GCA was relatively stable under our reaction conditions. And the isomerisation of GCA was enhanced by $LPMo_{12}$ in range of $AlPMo_{12}$ (Con. 43.1 % Y. 26.3 %) >$FePMo_{12}$ (37.5 %, 23.1 %)>$CrPMo_{12}$ (33.2 %, 19.0 %)> $TiPMo_{12}$ (24.0 %, 15.2 %) > $ZrPMo_{12}$ (19.5 %, 13.0 %)> $ZnPMo_{12}$ (12.1 %, 9.3 %) > $H_3PMo_{12}O_{40}$ (18.0 %, 6.0 %). The relationship between Lewis acidity and their activities was summarized in **Figure 4**, which determined that stronger Lewis acidity of POMs was main contribution to isomerisation of GCA to DHA. The same phenomenon was observed in $HPMo_{11}L$ system. The interaction between GCA and Al^{3+} was given in **scheme S1**, which contained four

Table 2. Isomerization of GCA to DHA being catalyzed by $LPMo_{12}$

Catalysts	Con of GCA, (%)	Yield of DHA (%)
$AlPMo_{12}$	43.1	26.3
$FePMo_{12}$	37.5	23.1
$CrPMo_{12}$	33.2	19.0
$TiPMo_{12}$	24.0	15.2
$ZrPMo_{12}$	19.5	13.0
$ZnPMo_{12}$	12.1	9.3
H_3PMo_{12}	18.0	6.0
No	10.0	4.3

Reaction conditions: 1.0 M of GCA, 4.0 mM of catalyst, 60 °C, 1 MPa of N_2, 800 rpm, 30 min.

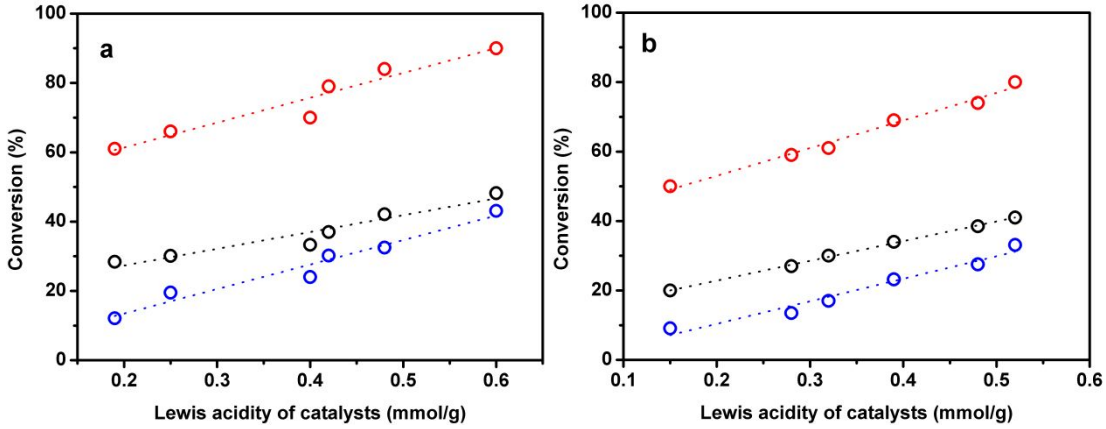

Figure 4. The relationship between the catalytic activity and Lewis acidity of $LPMo_{12}$ (a) and $HPMo_{11}L$ (b). The isomerization of GCA to DHA (blue), dehydration of DHA to PRA (black), and hydration of PRA to LA (red). Reaction conditions: 1.0 M of substrate, 4.0 mM of catalyst, 60 °C, 1 MPa of N_2, 800 rpm, 30 min.

reversible reactions and two resonances. This indicated that the existence of Lewis acidity for catalysts played pivotal role in isomerisation of GCA to DHA. (2) In dehydration of DHA to PRA (**Table 3**), the conversion of DHA depended on the Lewis acidity of $LPMo_{12}$. Meanwhile, there was some LA generated during dehydration reaction. (3) In hydration of PRA to LA (**Table 3**), Lewis acid presented almost the same effect on the activity as above two steps. In summary, Lewis acid exhibited a positive effect on the above three-step conversion. Nevertheless, these reactions showed the different rates as k (PRA → LA) > k (DHA → PRA) >> k (GCA → DHA), in which K = yield of products/reaction time. The pathway of GCA to DHA was supposed as the slowest step, which also called determine-rate step.

Table 3. Intermediate reactions being catalyzed by $LPMo_{12}$

Catalysts	Substrates	Conversion, %	Yield of PRA, %	Yield of LA, %
$AlPMo_{12}$	DHA	45.0	16.0	28.1
$FePMo_{12}$	DHA	42.1	14.3	26.3
$TiPMo_{12}$	DHA	37.0	10.0	24.2
$CrPMo_{12}$	DHA	33.3	9.1	23.1
$ZrPMo_{12}$	DHA	30.1	7.3	20.3
$ZnPMo_{12}$	DHA	28.4	6.0	19.0
$AlPMo_{12}$	PRA	90.0	-	88.1
$FePMo_{12}$	PRA	84.1	-	83.3
$TiPMo_{12}$	PRA	79.2	-	76.4
$CrPMo_{12}$	PRA	70.3	-	68.0
$ZrPMo_{12}$	PRA	66.1	-	63.2
$ZnPMo_{12}$	PRA	61.0	-	58.0

Reaction conditions: 1.0 M of substrates, 4.0 mM of catalyst, 60 °C, 1 MPa of N_2, 800 rpm,30 min.

After being treated at different temperature, the specific surface area of $AlPMo_{12}$-400 was almost7times higher than $AlPMo_{12}$-250 (**Table 1**), leading to a higher catalytic activity significantly (the glycerol conversion and LA yield were 98.6 and 96.1 % for $AlPMo_{12}$-400, 93.7 and 84.8 % for $AlPMo_{12}$-250), TOF of $AlPMo_{12}$-400 (35.2 h^{-1}) was also higher than $AlPMo_{12}$-250 (27.5 h^{-1}), which was almost the best yield of LA so far.[48] This phenomenon was also observed in $HPMo_{11}L/O_2$ system as $HPMo_{11}$Al-450 (con. 87.5 %) > $HPMo_{11}$Al-250 (78.0 %) > $HPMo_{11}$Al-150 (71.8 %) > $HPMo_{11}$Al-120 (65.2 %) > $HPMo_{11}$Al-orig (55.6 %), and $HPMo_{11}$Al-450 (Y. 70.3 %) > $HPMo_{11}$Al-250 (55.0 %) > $HPMo_{11}$Al-150 (44.2 %) > $HPMo_{11}$Al-120 (36.5 %) > $HPMo_{11}$Al-orig (28.0 %). These might be contributed to the enhancement in their specific surface areas as $HPMo_{11}$Al-450 (79.1 m^2/g)>$HPMo_{11}$Al-250 (20.1 m^2/g) > $HPMo_{11}$Al-150 (17.8 % m^2/g) > $HPMo_{11}$Al-120 (16.1 % m^2/g) > $HPMo_{11}$Al-orig (12.4 m^2/g) (**Table 1**). All the cases illustrated that the calcination treatment under different temperature can not only change the solubility of materials, but also improve their specific surface area, with more favour for catalytic transformation.

3. The influence of Lewis acidity and Brønsted acidity on glycerol conversion

At 2.2, the relationship between Lewis acidity and activity was studied. To investigate the difference between Brønsted and Lewis acid, $HPMo_{12}$, $Al_xH_{3-3x}PMo_{12}$ and $Fe_xH_{3-3x}PMo_{12}$ (x = 0.33, 0.67, 1.00) catalysts were synthesized, calcinated at 400 °C and applied in glycerol oxidation (**Figure 5**). As a typical Brønsted acid, $HPMo_{12}$ gave 54.2 % glycerol conversion and 30.1 % LA yield, indicating that the cascade reaction can be realized by the synergy of redox and Brønsted acid. For $Al_xH_{3-3x}PMo_{12}$ or $Fe_xH_{3-3x}PMo_{12}$, the relationship between B/L ratio and glycerol conversion was studied as $AlPMo_{12}$ (B/L = 0.1, 98.6 %), $Al_{0.67}HPMo_{12}$ ((B/L = 0.8, 84.0 %), $Al_{0.33}H_2PMo_{12}$ (B/L = 2.6, 70.1 %), and $FePMo_{12}$ (B/L = 0.1, 92.3 %), $Fe_{0.67}HPMo_{12}$ (B/L = 0.9, 78.0 %), $Fe_{0.33}H_2PMo_{12}$ (B/L = 3.5, 65.0 %) (**Table S7**). The higher the B/L value, the lower the glycerol conversion. The maximum values were both obtained at lowest B/L ratios for $AlPMo_{12}$ and $FePMo_{12}$, which was similar to our previous results in $Ag_xH_{3-x}PMo_{12}/O_2$ system. [14] The dehydration of DHA to PRA and hydration of PRA to LA catalyzed by $Al_xH_{3-3x}PMo_{12}$ and $Fe_xH_{3-3x}PMo_{12}$ were also studied (**Table 4**). The conversion of DHA and PRA decreased as the increase of B/L, and the maximum value of conversion was obtained by $AlPMo_{12}$ and $FePMo_{12}$ with B/L ratio of 0.1, showing that the Lewis acid preferred to improve the transformation of DHA and PRA. From the above result, it could be concluded that both the Brønsted and Lewis acidic sites can enhance the reaction rate of glycerol oxidation, while Lewis acidic sites played a main role.

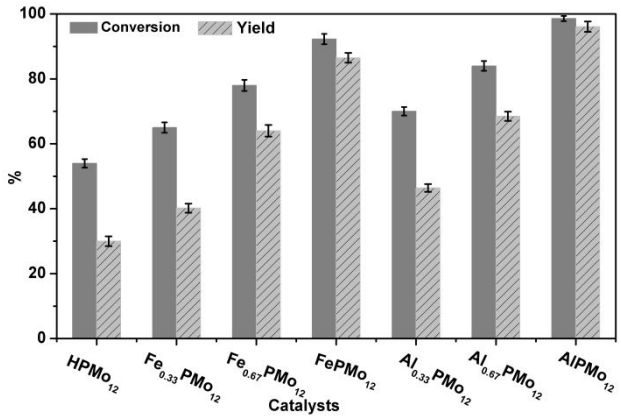

Figure 5. Glycerol oxidation activity of $HPMo_{12}$, Al_xPMo_{12}, and Fe_xPMo_{12} (x = 0.33, 0.67, and 1) after calcinated in 400 °C: 1 M glycerol, 4 mM catalyst, 60 °C, 5 h, 1 MPa O_2, 800 rpm.

The production distribution varied from the acidic nature of $Al_xH_{3-3x}PMo_{12}$ and $Fe_xH_{3-3x}PMo_{12}$. In dehydration of DHA reaction, $AlPMo_{12}$ and $FePMo_{12}$ gave the main product LA were 28.1 % and 26.3 %, respectively. Addition of Brønsted acidic catalysts, the LA yield dropped dramatically as $Al_{0.67}H_1PMo_{12}$ (21.3 %) > $Al_{0.33}H_2PMo_{12}$ (14.2 %), and $Fe_{0.67}H_1PMo_{12}$ (18.5 %) > $Fe_{0.33}H_2PMo_{12}$ (11.0 %) (**Table 4**). The same tracks were observed in rehydration of PRA, in which the yields of LA were $AlPMo_{12}$ (88.1 %) >

Table 4. Intermediate reactions being catalyzed by $Al_xH_{3-3x}PMo_{12}$ and $Fe_xH_{3-3x}PMo_{12}$

Catalysts	Substrates	Conversion, %	Yield of PRA, %	Yield of LA, %
$AlPMo_{12}$	DHA	45.0	16.0	28.1
$Al_{0.67}H_1PMo_{12}$	DHA	42.1	10.3	21.3
$Al_{0.33}H_2PMo_{12}$	DHA	40.3	5.0	14.2
$FePMo_{12}$	DHA	42.1	14.3	26.3
$Fe_{0.67}H_1PMo_{12}$	DHA	39.4	9.1	18.5
$Fe_{0.33}H_2PMo_{12}$	DHA	38.1	4.2	11.0
$AlPMo_{12}$	PRA	90.0	-	88.1
$Al_{0.67}H_1PMo_{12}$	PRA	88.5	-	73.3
$Al_{0.33}H_2PMo_{12}$	PRA	86.4	-	66.4
$FePMo_{12}$	PRA	84.1	-	83.3
$Fe_{0.67}H_1PMo_{12}$	PRA	76.8	-	63.1
$Fe_{0.33}H_2PMo_{12}$	PRA	73.0	-	48.0

Reaction conditions: 1.0 M of substrates, 4.0 mM of catalyst, 60 °C, 1 MPa of N_2, 800 rpm,30 min.

$Al_{0.67}H_1PMo_{12}$ (73.3 %) > $Al_{0.33}H_2PMo_{12}$ (66.4 %), and $FePMo_{12}$ (83.3 %) > $Fe_{0.67}H_1PMo_{12}$ (63.1 %) > $Fe_{0.33}H_2PMo_{12}$ (48.0 %). This indicated that Brønsted acidity did not favour for the generation of LA, which was contributed to the existence of side reaction to form some insoluble brown compounds.[49-50] Therefore, it can be concluded that the $L_xH_{3-3x}PMo_{12}$ catalysts with lowest B/L ratio had the highest selectivity for LA.

The hypothetical mechanism of catalysis by $AlPMo_{12}$ on the overall reaction of DHA to LA is showed in **Scheme 1**. In the reaction of DHA to PRA, cations act as Lewis acid catalysts through the keto-enoltautomerisation and subsequent dehydration by coordination to the carbonyl and hydroxyl groups. This mechanism was also proposed for the tin-catalyzed conversion of DHA in alcohols to alkyl lactate.[51] The reaction of the intermediate PRA to LA was shown to be catalyzed by Al ions, which is likely to involve hydration followed by a 1, 2-hydride shift.

4. Position of Lewis metals on the pathways for glycerol conversion

Two types of POMs, Lewis metals as counter ions and addenda atoms, gave different catalytic activities in glycerol oxidation (**Figure 6**). Metal exchanged phosphomolybdate $AlPMo_{12}$ showed higher conversion of glycerol (93.7 %) than metal in addenda position $HPMo_{11}Al$ (78.1 %) did. Apparently, such difference

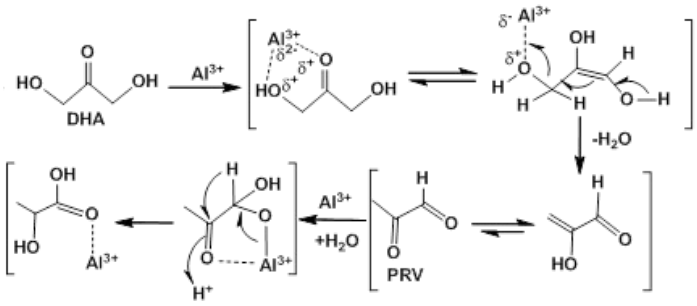

Scheme 1.The mechanism of DHA transformation to LA in the presence of Al^{3+}.

was attributed to the position of Lewis metal ions in POMs, which $AlPMo_{12}$ presented higher Lewis acidity than $HPMo_{11}Al$ did. At the beginning of the reaction, glycerol conversion catalyzed by $HPMo_{11}Al$ was higher than that catalyzed by $AlPMo_{12}$ as well as yields of DHA and GCA, which was caused by their variety in redox potentials. From the H_2-TPR results (**Figure 3**), the oxidative ability of $AlPMo_{12}$ (3.5×10^{-6} mol/mol) was lower than that of $HPMo_{11}Al$ (5.3×10^{-6} mol/mol), which was similar as that being reported by Hill, Mizuno and others.[52-54] The symmetry of the POM molecules was destroyed after one addendum atom Mo or W was replaced by other metal ions, which lead to increasing in the redox ability compared to the original keggin POMs. The yield of LA catalyzed by $AlPMo_{12}$ was always higher than that by $HPMo_{11}Al$. Based on our previous investigation, there may be two main reasons: one is the Lewis acidity of $AlPMo_{12}$ (0.60 mmol/g) is higher than that of $HPMo_{11}Al$ (0.52 mmol/g), which prefer to improve the formation of intermediates including DHA, PRA and finally LA, without any side reactions. The second reason would be that Brønsted acidity might give rise to more side reactions to reduce the LA yield.[49-50]

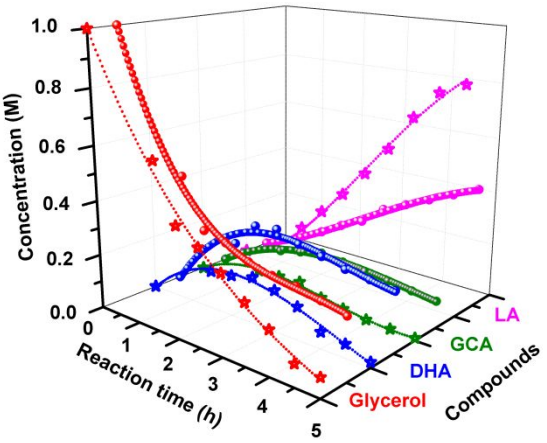

Figure 6. Glycerol oxidation reaction catalyzed by $AlPMo_{12}$ (pentagram) and $HPMo_{11}Al$ (circle): 1 M of glycerol, 4 mM of catalyst, 60 °C, 1 MPa of O_2, 800 rpm.

To determine the different influence of position of Lewis metal, the individual reactions involved in glycerol oxidation were done upon $AlPMo_{12}$ and $HPMo_{11}Al$ (**Table 5**). For the glycerol dehydrogenation oxidation, the glycerol oxidation catalyzed by $AlPMo_{12}$ was lower than $HPMo_{11}Al$ at the beginning of the reaction (30 min), which was attributed to the difference of their redox capability: For the isomerization of GCA to DHA, $AlPMo_{12}$ showed higher activity than $HPMo_{11}Al$ did due to stronger influence on acidity in counter ion position than in addenda position. Al^{3+} as counter ion was in tetrahedral position outside the polyanion, which allowed it show high Lewis acidity. In $HPMo_{11}Al$, Al^{3+} was in octahedral position surrounded by oxygen, which was difficult to release Lewis acidity. The similar tracks were obtained in the dehydration of DHA to PRA and hydration of PRA to LA as well, which also determined the essential of Lewis acid sites. Meanwhile, the mass balance of the products catalyzed by $AlPMo_{12}$ was all higher than that by $HPMo_{11}Al$, which was supposed to be the existence of Brønsted acid was main contribution to generation of some insoluble brown products, which might decrease the production of DHA for consequent conversion.[49-50]

Table 5. Oxidation of glycerol in the presence of $AlPMo_{12}$ and $HPMo_{11}Al$ catalysts

Entry	Catalyst	substrates	CON%	Yield, %				
				DHA	GCA	PRA	LA	Mass balance (%)
1	$AlPMo_{12}$	Glycerol	22.0	13.0	6.0	1.0	1.0	95.4
2	$HPMo_{11}Al$	Glycerol	31.0	18.0	8.0	1.0	1.0	90.3
3	$AlPMo_{12}$	GCA	43.1	26.3	-	9.2	5.1	97.5
4	$HPMo_{11}Al$	GCA	25.0	15.2	-	6.3	2.3	92.0
5	$AlPMo_{12}$	DHA	45.0	-	1.2	16.0	28.1	95.5
6	$HPMo_{11}Al$	DHA	28.0	-	1.1	15.1	10.2	92.8
7	$AlPMo_{12}$	PRA	90.0	-	-	-	88.1	98.9
8	$HPMo_{11}Al$	PRA	79.0	-	-	-	74.1	93.6

Reaction conditions: 1 M glycerol, 4mM catalyst, 60 °C, 30min, 1 MPa O_2, 800 rpm.

5. Conversion of neat glycerol and crude glycerol

To the best of our knowledge, neat glycerol was difficult to be converted because of thestrong hydrogen bond. Interestingly, $AlPMo_{12}$-400 performed excellent in this strict transformation (LA yield was 84.1 % at the 71.8 % glycerol conversion) under mild conditions (1 MPa O_2, 800 rpm, 60 °C, 24 h). As the main by-products at biodiesel production, crude glycerol was not easy to be converted owing to the impurity, which was usually negatively influence the catalytic upgrading of glycerol.[55-57]To investigate the efficiency of our catalyst, we use mixture of 71 wt % glycerol, 28 wt % methanol, and other minor organic chemicals to simulate the crude glycerol. Surprisingly, $AlPMo_{12}$-400 displayed good activity in converting crude glycerol to LA with the glycerol conversion of 92.1 % and LA yield of 86.8 % under mild conditions (1 M of crude glycerol solution, 4.0 mM of $AlPMo_{12}$-400, 1 MPa O_2, 60 °C, 5 h). This result suggests $AlPMo_{12}$-400 to be a methanol-tolerant catalyst capable of converting crude glycerol.

6. Reusability of POMs

$AlPMo_{12}$ and $HPMo_{11}Al$ were successfully reused for 12 times without significant loss of catalytic activity and selectivity for LA formation (**Figure 7**). After each catalytic run, the catalyst was recovered by centrifugation, washed with ethanol and dried before reuse. The IR spectra, ^{31}PMAS NMR, and powder X-ray diffraction (XRD) of the used materials did not show some difference compared to the fresh ones, indicating that the structure of the heteropolyanion remained intact (**Figure S13-16**). $AlPMo_{12}$ and $HPMo_{11}Al$ presented higher stability and duriation. The loss amount of catalyst was mainly contributed to the little solubility in water. The loss amount of POMs in the mixture solution after reaction was tested by UV-Vis spectroscopy, which reached to 5.2 % after 12 recycles to determine their insolubility in water.

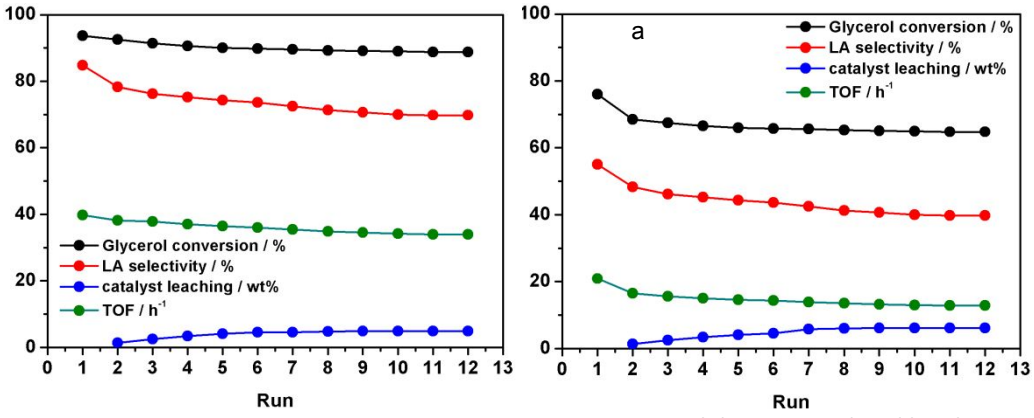

Figure7. Reusability test catalyzed by $AlPMo_{12}$ (a) and $HPMo_{11}Al$ (b) in oxidation reaction of glycerol.Reaction condition:1 M glycerol, 4 mM catalysts, 60 °C, 1 MPa O_2, 5 h, 800 rpm. TOF use the initial rates.

Furthermore, a hot catalyst filtration test [58] was carried out to verify the truly heterogeneous nature of the catalysis (**Figure S17**). Catalyst was filtered from the reaction mixture after 2 h, and the filtrate was

allowed to react for5 h to clarify whether there were some catalysts leaching into the reaction mixture. Then the reaction mixture was analyzed by HPLC. It was found that the conversion of glycerol was not significantly improved as 60.6 % after hot filtration compared to the previous result (93.7 %). This result indicated that there was no leaching of $AlPMo_{12}$ into the reaction mixture at 60 °C. Therefore, $AlPMo_{12}$ acted as a heterogeneous catalyst in the glycerol oxidation.

Conclusions

A serious of solid POMs as $LPMo_{12}$ (L = Al^{3+}, Fe^{3+}, Cr^{3+}, Ti^{4+}, Zr^{4+}, and Zn^{2+}) and $HPMo_{11}L$ (L= Zn^{2+}, Cr^{3+}, Fe^{3+}, Al^{3+}, Ti^{4+}, for Ti^{4+}, the amount of O is 40) was synthesized through simple calcination treatment. After being treated at 400 °C, mesoporous structure with high specific surface area was built without distortion. These two POMs were evaluated in glycerol transformation to LA in the presence of O_2. special active sites of redox, Lewis acid, and Brønsted acid might play different role on each step containing oxidation of glycerol by redox sites, isomerization of GCA to DHA, and dehydration/hydration of DHA to LA via PRA intermediate by Lewis acidic sites. The position of metal ion first influenced their redox potential to allow $HPMo_{11}Al$ exhibit higher oxidation ability than $AlPMo_{12}$; secondly, metals in counter ion position gave rise to higher effect on Lewis acidity for POMs, and LA yield was improved as well. Meanwhile, the existence of Brønsted acid could decrease the LA yield due to side-reactions. Among all, $AlPMo_{12}$-400 was found to be the most active one with 96.1 % yield of LA at 98.6 % glycerol conversion at mild reaction conditions as 60 °C for 5 h, which was almost the best yield and selectivity so far in this field. $AlPMo_{12}$-400 also performed excellently in the conversion of crude glycerol (LA yield was 86.8 % within 5 h) and neat glycerol (LA yield was 84.1 % with 24 h).$AlPMo_{12}$ and $HPMo_{11}Al$ remained stable after being reused 12 times without significant leaching into the solution. The method for heterogenization of soluble POMs and catalytic activity in glycerol conversion provided a new alternative for POM in applications.

Conflicts of interest

There are no conflicts to declare.

Acknowledgements

We thank the National Natural Science Foundation of China (51978134) and Jilin Provincial Science and Technology Department (20180414069GH). And the Department of Energy, Office of Basic Energy Sciences, Solar Photochemistry program, grant number DE-FG02-07ER15906 and the China scholarship council for support of this research.

List of the abbreviations

$H_3PMo_{12}O_{40}$ as $HPMo_{12}$; $Al_3PMo_{12}O_{40}$ as $AlPMo_{12}$; $FePMo_{12}O_{40}$ as $FePMo_{12}$; $CrPMo_{12}O_{40}$ as $CrPMo_{12}$; $Ti_{0.75}PMo_{12}O_{40}$ as $TiPMo_{12}$; $Zr_{0.75}PMo_{12}O_{40}$ as $ZrPMo_{12}$; $Zn_{1.5}PMo_{12}O_{40}$ as $ZnPMo_{12}$; $Al_{0.33}H_2PMo_{12}O_{40}$ as $Al_{0.33}PMo_{12}$; $Al_{0.67}H_1PMo_{12}O_{40}$ as $Al_{0.67}PMo_{12}$; $Fe_{0.33}H_2PMo_{12}O_{40}$ as $Fe_{0.33}PMo_{12}$; $Fe_{0.67}H_1PMo_{12}O_{40}$ as $Fe_{0.67}PMo_{12}$; dihydroxyacetone as DHA; glyceraldehyde as GCA; pyruvaldehyde as PRA; lactic acid as LA; $H_4PMo_{11}AlO_{39}$ as $HPMo_{11}Al$; $H_4PMo_{11}FeO_{39}$ as $HPMo_{11}Fe$; $H_4PMo_{11}CrO_{39}$ as $HPMo_{11}Cr$; $H_5PMo_{11}ZnO_{39}$ as $HPMo_{11}Zn$; $H_5PMo_{11}TiO_{40}$ as $HPMo_{11}Ti$.

Notes and references

1 M. Tao, L. Xue, Z. Sun, S. Wang, X. Wang and J. Shi, *Sci. Rep.* 2015, **5**, 1.
2 K. Suzuki, M. Sugawa, Y. Kikukawa, K. Kamata, K. Yamaguchi and N. Mizuno, *Inorg. Chem*. 2012, **51**, 6953.
3 C. Boglio, K. Micoine, P. Remy, B. Hasenknopf, S. Thorimbert, E. Lacôte, M. Malacria, C. Afonso and J. C. Tabet, *Chem Eur. J.* 2007, **13**, 5426.
4 Y. Kikukawa, S. Yamaguchi, K. Tsuchida, Y. Nakagwa, K. Uehara, K. Yamaguchi and N. Mizuno, *J. Am. Chem. Soc*. 2008, **130**, 5472.
5 Y. Kikukawa, S. Yamaguchi, Y. Nakagawa, K. Uehara, S. Uchida, K. Yamaguchi and N. Mizuno, *J. Am. Chem. Soc*. 2008, **130**, 15872.
6 M. Bosco, S. Rat, N. Dupre, B. Hasenknopf, E. Lacote, M. Malacria, P. Remy, J. Kovensky, S. Thorimbert and A. Wadouachi, *ChemSusChem*. 2010, **3**, 1249.
7 S. S. Wang and G. Y. Yang, *Chem. Rev*. 2015, **115**, 4893.
8 S. A. Zavrazhnov, A. L. Esipovich, S. M. Danov, S. Y. Zlobin, and A. S. Belousov, *Kinet. Catal*. 2018, **59**, 459.

9 S.Carrettin, P.McMorn, P. Johnston, K. Griffin, C. J. KielycandG. J. Hutchings, *Phys. Chem. Chem. Phys.*, 2003, **5**, 1329.
10 P.McMorn, G. Roberts and G. J. Hutchings, Catal Lett. 1999, **63**, 193.
11 N. Dimitratos, C. Messi, F. Porta, L. Prati, A. Villa, J Mole Catal A: Chem. 2006, **256**, 21.
12 F. Porta and L.Prati, J Catal. 2004, **224**, 397.
13 A. Villa, S.Campisi, K. M. H. Mohammed, N. Dimitratos, F.Vindigni, M.Manzoli, W. Jones, M. Bowker, G. Hutchings, and L.Prati, Catal. Sci. Technol., 2015,**5**, 1126.
14 M. Tao, D. Zhang, H. Guan, G. Huang and X. Wang, *Sci. Rep*. 2016, **6**,1.
15 M. Tao, D. Zhang, X. Deng, X. Li, J. Shi and X. Wang, *Chem. Commun*. 2016, **52**, 3332.
16 M. Tao, Y. Li, Y. V. Geletii, C. L. Hill, and X. Wang, *Appl. Catal A: Gen.* 2019, **579**, 52.
17 M. Tao, X. Yi, I. Delidovich, R. Palkovits, J. Shi, and X. Wang, *ChemSusChem*. 2015, **8**, 4195.
18 M. Tao, N. Sun, Y. Li, T. Tong, M. Wielicako, S. Wang and X. Wang, *J. Mater. Chem. A*. 2017, **5**, 8325.
19 M. Tao, Y. Li, X. Zhang, Z. Li, C. L. Hill, and X. Wang, *ChemSusChem*. 2019, **12**, 1.
20 M. Tao, N. Sun, Y. Li, S. Wang and X. Wang, *Catal. Sci. Technol*. 2020, **10**, 207.
21 A. E. Kerenkan, T. O. Do and S. Kaliaguine, *Catal. Sci. Technol*. 2018, **8**, 2257.
22 PutlaSudarsanam, Ruyi Zhong, Sander Van den Bosch, Simona M. Coman, Vasile I. Parvulescu, and Bert F. Sels, *Chem. Soc. Rev*., 2018,**47**, 8349.
23 N. Mizuno and M.Misono, *Chem. Rev*. 1998, **98**, 199.
24 S. S. Wang, G. Y. Yang, *Chem. Rev*. 2015, **115**, 4893.
25 A. Enferadi-Kerenkan, T. O. Do and S. Kaliaguine, *Catal. Sci. Technol*. 2018, **8**, 2257.
26 Y. Zhou, G. Chen, Z. Long and J. Wang. *RSC Adv*. 2014, **4**, 42092.
27 O. Toshio, N. ToruandM. Makoto, *Chem. Lett*. 1995, **24**, 155.
28 L. Yang, L. W. Xu and C. G. Xia, *Tetrahedron. Lett.* 2008, **49**, 2882.
29 T. H. T.Vu, H. T.Au, T. M. T. Nguyen, M. T. Pham, T. T. Bach and H. N. Nong, *Catal. Sci. Technol*. 2013, **3**, 699.
30 C. R. Kumar, K. T. V. Rao, P. S. S. Prasad and N. Lingaiah, *J. Mol. Catal A: Chem*. 2011, **337**, 17.
31 J. Li, X. Wang, W. Zhu and F. Cao, *ChemSusChem*. 2009, **2**, 177.
32 J. Wang, G. Luo, C. Liu and J. Lai, *Energy. Sources. Part. A*. 2014, **36**, 479.
33 N. R. Shiju, A. H. Alberts, S. Khalid, D. R. Brown and G. Rothenberg, *Angew. Chem. Int. Ed.* 2011, **123**, 9789.
34 K. Inumaru, T. Ishihara, Y. Kamiya, T. Okuhara and S. Yamanaka, *Angew. Chem. Int. Ed*. 2007, **46**, 7625.
35 F. Su, L. Ma, Y. Guo and W. Li, *Catal. Sci Technol*. 2012, **2**, 2367.
36 J. Sloan, Z. Liu, K. Suenaga, N. R. Wilson, P. A. Pandey, L. M. Perkins, J. P. Rourke and I. J. Shannon, *Nano. Lett.* 2010, **10**, 4600.
37 I. A. Weinstock, R. H. Atalla, R. S. Reiner, C. J. Houtman and C. L. Hill, *Holzforshung*. 1998, **52**, 304.
38 S. Borghèse, B. Louis, A. Blanc and P. Pale, *Catal. Sci Technol.* 2011, **1**, 981.
39 S. Borghèse, A. Blanc, P. Pale and B. Louis, *Dalton Trans.* 2011, **40**, 1220.
40 T. Mazari, C. R. Marchal, S. Hocine, N. Salhiand C. Rabia, *J. Nat Gas Chem*. 2009, **18**, 319.
41 S. Kendell and T. Brown, *Reac. Kinet. Mech. Cat.* 2010, **99**, 251.
42 S. Tei, M. Hirotoshi, S. Tatsuya, F. Yasuhiko, and K. Kiyoshi, *J. PlasmaFusion Res.*2002,**78**,1.
43 F. Jing, B.Katryniok, F.Dumeignil, E.Bordes-Richard, S. Paul, *J Catal*. 2014, **309**, 121.
44 Y. Liu, J. He, W. Chu, W. Yang, *Catal. Sci. Technol.*, 2018,**8**, 5774.
45 M. C. Ávila, N. A. Comelli, E. Rodríguez-Castellón, A. Jiménez-López, R. C. Flores, E. N. Ponzi and M. I. Ponzi, *J. Mol. Catal. A: Chem.* 2010, **322**, 106.
46 S. Liang, G. B. Hammond and B. Xu, *Chem. Commun*. 2015, **51**, 903.
47 C. A. Emeis, *J Catal*. 1993, **141**, 347.
48 N. Razali and A. Z. Abdullah, *Appl. Catal. A: Gen*. 2017, **543**, 234.
49 C. B. Rasrendra, B. A. Fachri, I. G. B. N. Makertihartha, S. Adisasmito and H. J. Heeres, *ChemSuschem*. 2011, **4**, 768.
50 T. Komanoya, A. Suzuki, K. Nakajima, M. Kitano, K. Kamata and M. Hara, *ChemCatChem*. 2016, **8**, 1094.
51 Y. Hayashi and Y. Sasaki, *Chem. Commun*. 2005, **0**, 2716.
52 N. Mizuno, J. S. Min and A. Taguchi, *Chem. Mater*. 2004, **16**, 2819.
53 L. A. Combs-Walker and C. L. Hill, *Inorg. Chem*. 1991, **30**, 4016.
54 Y. Zhang, Y. Gu, X. Dong, P. Wu, Y. Li, H. Hu and G. Xue, *Catal. Lett*. 2017, **147**, 1811.
55 L. S. Sharninghausen, J. Campos, M. G. Manas and R. H. Crabtree, *Nat. Commun*. 2014, **5**, 5084.
56 E. Skrzyn´ska, A. Wondołowska-Grabowska, M. Capron and F. Dumeignil, *Appl. Catal. A* 2014, **482**, 245.

57 F. Yang, M. Hanna and R. Sun, *Biotechnol. Biofuels*. 2012, **5**, 13.
58 R. A. Sheldon,M.Wallau,I. W. C. E. Arends, and U.Schuchardt, *Acc. Chem. Res.* 1998, **31**, 485.

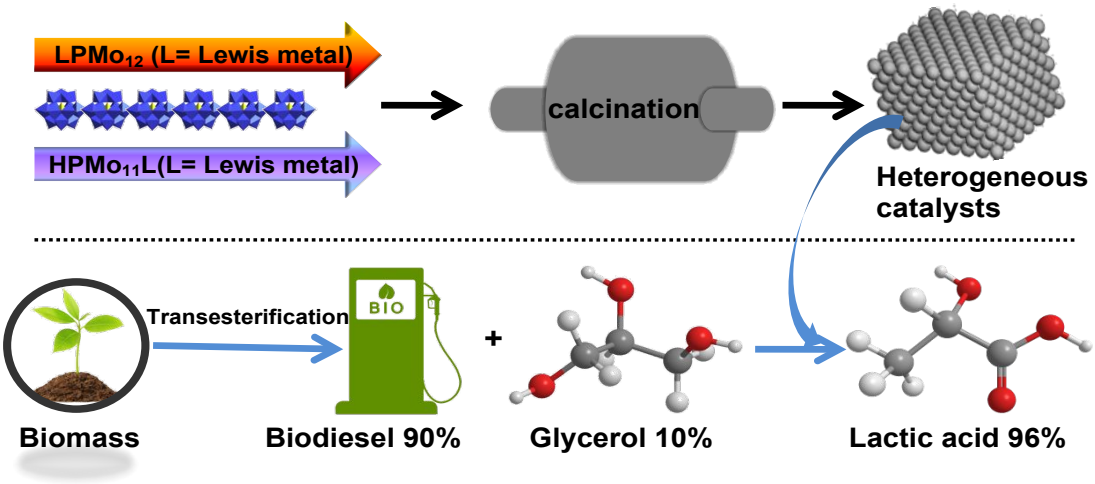
LPMo12 (L= Lewis metal)
HPMo11L(L= Lewis metal)
calcination
Heterogeneous catalysts
Transesterification
BIO
+
Biomass
Biodiesel 90%
Glycerol 10%
Lactic acid 96%